

# Advances in analyses of three-body decays

Mikhail Mikhasenko

CERN, Switzerland

LHCb Collaboration  
JPAC Collaboration

April 14<sup>th</sup>, 2021

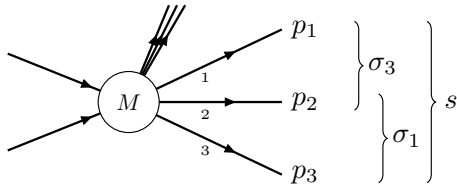


# The plan for the talk

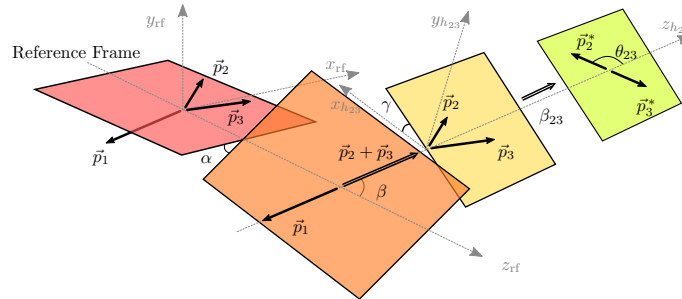
- 1 Search for CPV in  $\Xi_b^- \rightarrow p K^- K^-$
- 2 Lineshape analysis for  $\Lambda_b^{**0} \rightarrow \Lambda_b^0 \pi^+ \pi^-$

# Three-body problem in HEP

$$M = M(\alpha, \beta, \gamma, s, m_{12}^2, m_{23}^2)$$



- $s$  is a total invariant mass. **3b dynamics**
- $\sigma_3 \equiv m_{12}^2 \times \sigma_1 \equiv m_{23}$ . **Dalitz plot**
- $(\alpha, \beta, \gamma)$  decay plane orientation. **Euler**

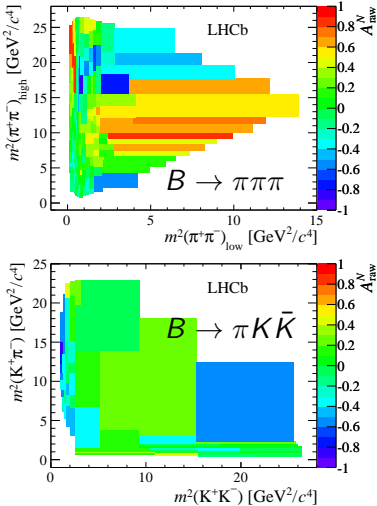


# Amplitude analysis of $\Xi_b^- \rightarrow p K^- K^-$

[LHCb-PAPER-2020-017 (NEW! in preparation)]

# CP violation in hadronic decays

CPV is well seen in  $B \rightarrow hhh$ :



[PRD 90, 112004 (2014)]

Appearance of CPV effects:

$$B \rightarrow f : \quad A = \sum_i |A_i| e^{i(\delta_i + \phi_i)}$$

$$\bar{B} \rightarrow \bar{f} : \quad \bar{A} = \sum_i |A_i| e^{i(\delta_i - \phi_i)},$$

- Strong phase ( $\delta$ ) does not change under CP,
- Weak phase ( $\phi$ ) flip the sign.

$$\mathcal{A}_{\text{CP}} = \frac{|A|^2 - |\bar{A}|^2}{|A|^2 + |\bar{A}|^2}$$

$$\rightarrow \sum_i |A_i| |A_j| \sin(\delta_i - \delta_j) \sin(\phi_i - \phi_j)$$

**NOTHING**  
in baryonic decays

In  $\Lambda_b^0$  decay:

- $pK^-$ ,  $p\pi^-$ ,  
 $K_S^0 p\pi^-$ ,  $\Lambda K^- K^+$
- $p\pi^- \pi^- \pi^+$ ,  
 $p\pi^- K^- K^+$ ,  
 $pK^- \pi^+ \pi^+$ ,  
 $pK^- K^+ K^+$

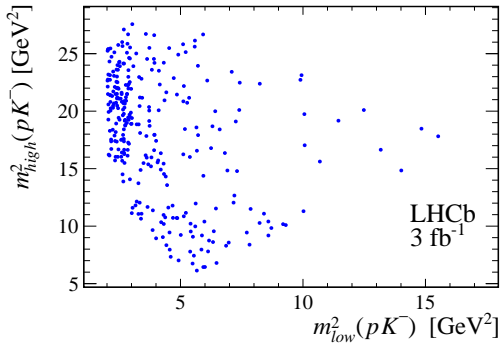
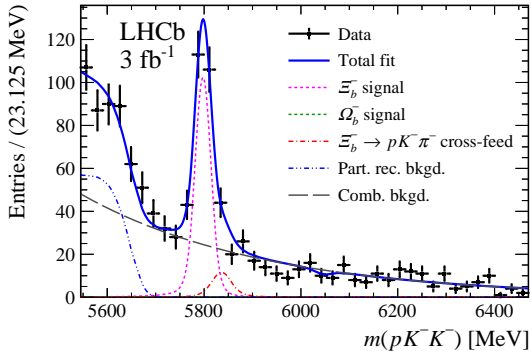
In  $\Xi_b^-$  decay:

- $pK^- \pi^+ \pi^+$ ,  
 $pK^- \pi^+ K^+$

?  $pK^- K^-$

# Observation of $\Xi_b^- \rightarrow p K^- K^-$ decay

[LHCb-PAPER-2020-017]

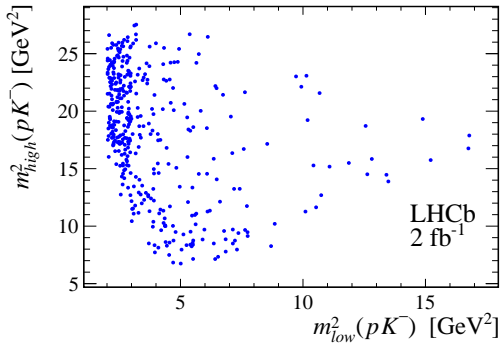
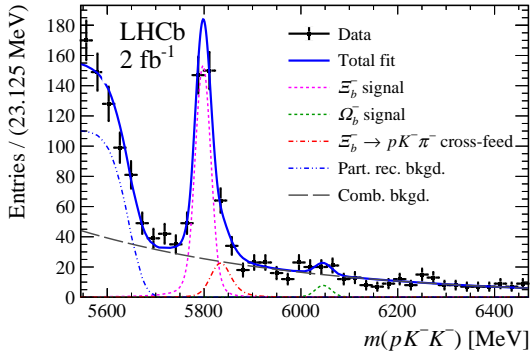


- Run I + a part of Run II  $\Rightarrow 5 \text{ fb}^{-1}$ .
- 460 signal candidates,
  - + combinatorial background,
  - +  $\Xi_b^- \rightarrow p K^- K^-$  misidentification.

- $K^-K^-$  symmetry makes Dalitz plot (double entry) symmetric
- Only half is analysed (single entry)

# Observation of $\Xi_b^- \rightarrow p K^- K^-$ decay

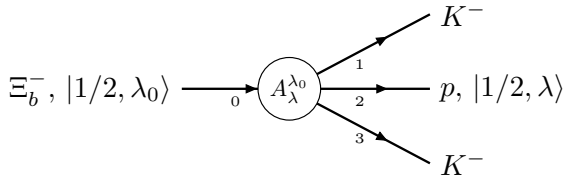
[LHCb-PAPER-2020-017]



- Run I + a part of Run II  $\Rightarrow 5 \text{ fb}^{-1}$ .
- 460 signal candidates,
  - + combinatorial background,
  - +  $\Xi_b^- \rightarrow p K^- K^-$  misidentification.

- $K^- K^-$  symmetry makes Dalitz plot (double entry) symmetric
- Only half is analysed (single entry)

## $\Xi_b^-$ decay amplitude



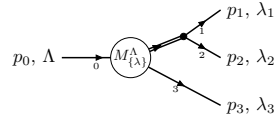
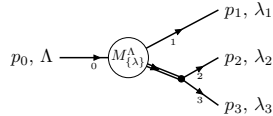
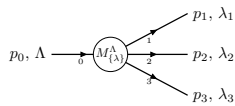
- Baryon decay (half-integer spin)  
⇒  $4\pi$ -fold azimuthal symmetry of the decay amplitude
- Two identical kaons in the final state  
⇒ Symmetry of the decay amplitude.
- Intermediate  $\Sigma, \Lambda$  states decaying to  $pK^-$

# Conventional helicity approach

Complicated cases: particles with spin in isobar model [Hansen (1974)], [Herndon(1975)]

$$M_{\{\lambda\}}^{\Lambda} = M_{1,\{\lambda\}}^{\Lambda} + M_{2,\{\lambda\}}^{\Lambda} + M_{3,\{\lambda\}}^{\Lambda}$$

$$\underbrace{M_{\{\lambda\}}^{\Lambda}}_{= H_1 D(\phi_1, \theta_1, 0) D(\phi_{23}, \theta_{23}, 0) W_1(\dots)} + \underbrace{H_3 D(\phi_3, \theta_3, 0) D(\phi_{12}, \theta_{12}, 0) W_3(\dots)}$$

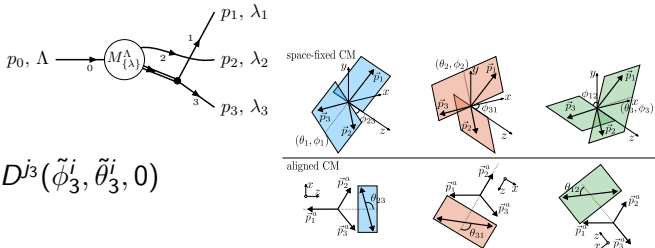


$$+ \underbrace{H_2 D(\phi_2, \theta_2, 0) D(\phi_{31}, \theta_{31}, 0) W_2(\dots)}$$

- A special set of angles for every decay chain
- Consistently of quantization direction – **Wigner rotations**

$$W_i(\dots) = D^{j_1}(\tilde{\phi}_1^i, \tilde{\theta}_1^i, 0) D^{j_2}(\tilde{\phi}_2^i, \tilde{\theta}_2^i, 0) D^{j_3}(\tilde{\phi}_3^i, \tilde{\theta}_3^i, 0)$$

- Fails for non-integer spin



# The Dalitz-Plot decomposition

[MM et al.(JPAC), PRD 101, 034033 (2020)]

Reformulation of the helicity approach

Feynman diagram illustrating the decay of a  $\Lambda$  baryon into three particles. An incoming particle  $p_0, \Lambda$  with index 0 enters a vertex labeled  $M_{\{\lambda\}}^{\Lambda}$ . From this vertex, three outgoing particles emerge:  $p_1, \lambda_1$  with index 1,  $p_2, \lambda_2$  with index 2, and  $p_3, \lambda_3$  with index 3.

$$p_0, \Lambda \xrightarrow{0} M_{\{\lambda\}}^{\Lambda} \begin{cases} p_1, \lambda_1 \\ p_2, \lambda_2 \\ p_3, \lambda_3 \end{cases} = \sum_{\nu} \underbrace{D_{\Lambda\nu}^{J*}(\phi_1, \theta_1, \phi_{23})}_{\text{Decay-plane orientation}} \times \underbrace{O_{\{\lambda\}}^{\nu}(\{\sigma\})}_{\text{Dalitz-plot function}}$$

Model-independent factorization of the overall rotation:

- Exploits properties of the Lorentz group (orientation – just three Euler angles)
- Dalitz-plot function depends entirely on 2 variables,  $\{\sigma\} \equiv \{\sigma_1, \sigma_2, \sigma_3\}$
- No azimuthal phase factors in  $O_{\{\lambda\}}^{\nu}$ .

Gives significant benefits to

- Pentaquark analysis,  $\Lambda_b/\Lambda_c$  polarionation measurements, Baryonic decay chains,...

# Dalitz-Plot function

[MM et al.(JPAC), arXiv:1910.04566]

Master formula  $0 \rightarrow 123$  decay with arbitrary spins

$$O_{\{\lambda\}}^{\nu}(\{\sigma\}) = \sum_{(ij)k} \sum_s^{(ij) \rightarrow i,j} \sum_{\tau} \sum_{\{\lambda'\}} n_J n_s d_{\nu, \tau - \lambda'_k}^J(\hat{\theta}_{k(1)}) X_s^{\tau, \lambda'_k; \lambda'_i, \lambda'_j}(\sigma_k) d_{\tau, \lambda'_i - \lambda'_j}^s(\theta_{ij}) \\ \times d_{\lambda'_1, \lambda_1}^{j_1}(\zeta_{k(0)}^1) d_{\lambda'_2, \lambda_2}^{j_2}(\zeta_{k(0)}^2) d_{\lambda'_3, \lambda_3}^{j_3}(\zeta_{k(0)}^3),$$

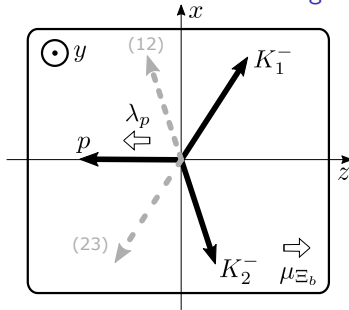
- Three decay chains,  $(ij)k \in \{(12)3, (23)1, (31)2\}$ .
- $\theta_{ij} = \theta_{ij}(\{\sigma\})$  is an isobar decay angle
- $\hat{\theta}_{k(1)} = \hat{\theta}_{k(1)}(\{\sigma\})$  is the particle-0 Wigner angle
- $\zeta_{k(0)}^i = \zeta_{k(0)}^i(\{\sigma\})$  is the particle- $i$  Wigner angle

Applied in LHCb

- $P_c$  in  $\Lambda_b^0 \rightarrow J/\psi p K^-$
- $P_{cs}$  in  $\Xi_b^- \rightarrow J/\psi \Lambda^0 K^-$
- $\Lambda_c^+ / \Xi_c^+ \rightarrow p K^- \pi^+$
- Some analyses in progress

Symmetrization:  $(K^- p) K^- + K^- \underbrace{(pK^-)}_{\text{low}}$   $\underbrace{(K^- p)}_{\text{high}}$

[LHCb-PAPER-2020-017]



$$A_{\lambda_0, \lambda} = \sum_{\nu} D_{\lambda_0, \nu}^{1/2}(\alpha, \beta, \gamma) O_{\lambda}^{\nu}(m_{\text{high}}^2, m_{\text{low}}^2)$$

The helicity amplitude with explicit permutation symmetry:

$$O_{\lambda}^{\nu} = T_{\lambda}^{\nu}(m_{\text{high}}^2, m_{\text{low}}^2) \quad \boxed{+} \quad (-1)^{\nu+\lambda} T_{\lambda}^{\nu}(m_{\text{low}}^2, m_{\text{high}}^2)$$

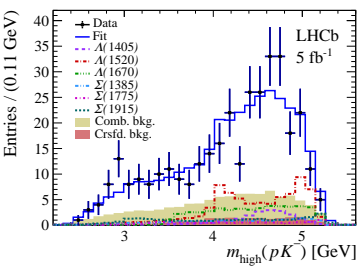
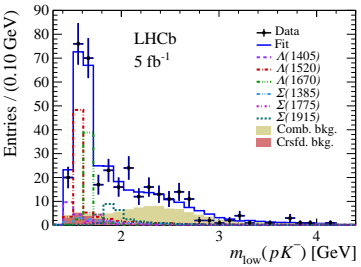
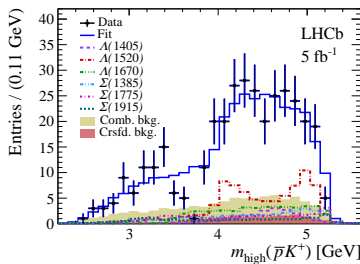
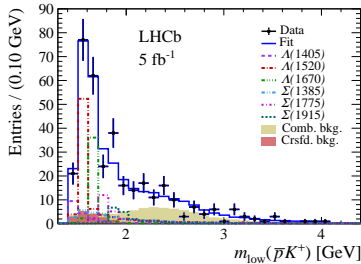
$T_{\lambda}^{\nu}$  is the resonance decay amplitude  $\Xi_b^- \rightarrow R^0 (\rightarrow K^- p) K^-$ .

$(-1)^{\nu+\lambda}$ : permutation of kaons  $K_1^- \leftrightarrow K_3^-$  flips the  $x$ - $z$  plane  $\Rightarrow R_z(\pi)$

Clearly  $\boxed{+}$  in covariant:  $A = \bar{u}(p, \lambda) \left[ \frac{\not{p}_{R_1} + m_{\text{high}}}{2m_{\text{high}}^2} + \frac{\not{p}_{R_3} + m_{\text{low}}}{2m_{\text{low}}^2} \right] u(p_b, \nu) \Rightarrow \text{check!}$

# Fit to $\Xi_b^- \rightarrow pK^-K^-$ . CP test!

[LHCb-PAPER-2020-017]



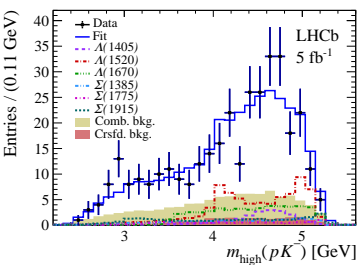
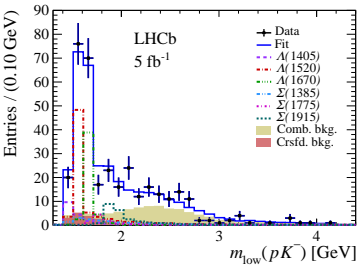
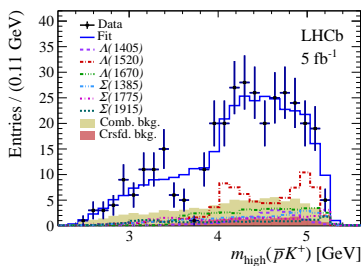
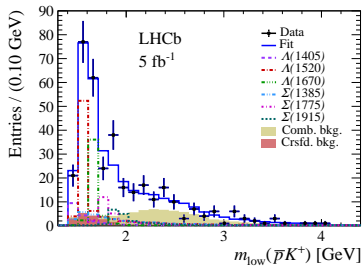
## Fractions:

$$\begin{aligned}\Sigma(1385) &\rightarrow 0.26(11)(17) \\ \Lambda(1405) &\rightarrow 0.19(6)(7) \\ \Lambda(1520) &\rightarrow 0.76(9)(8) \\ \Lambda(1670) &\rightarrow 0.45(7)(13) \\ \Sigma(1775) &\rightarrow 0.22(8)(9) \\ \Sigma(1915) &\rightarrow 0.26(9)(21)\end{aligned}$$

errors: (stat.)(syst.)

# Fit to $\Xi_b^- \rightarrow pK^-K^-$ . CP test!

[LHCb-PAPER-2020-017]



## Fractions:

$$\begin{aligned}\Sigma(1385) &\rightarrow 0.26(11)(17) \\ \Lambda(1405) &\rightarrow 0.19(6)(7) \\ \Lambda(1520) &\rightarrow 0.76(9)(8) \\ \Lambda(1670) &\rightarrow 0.45(7)(13) \\ \Sigma(1775) &\rightarrow 0.22(8)(9) \\ \Sigma(1915) &\rightarrow 0.26(9)(21)\end{aligned}$$

errors: (stat.)(syst.)

## Asymmetries $A_{\text{CP}} \times 10^{-2}$ :

$$\begin{aligned}\Sigma(1385) &\rightarrow -27(34)(73) \\ \Lambda(1405) &\rightarrow -1(24)(32) \\ \Lambda(1520) &\rightarrow -5(9)(8) \\ \Lambda(1670) &\rightarrow +3(14)(10) \\ \Sigma(1775) &\rightarrow -47(26)(14) \\ \Sigma(1915) &\rightarrow +11(26)(22)\end{aligned}$$

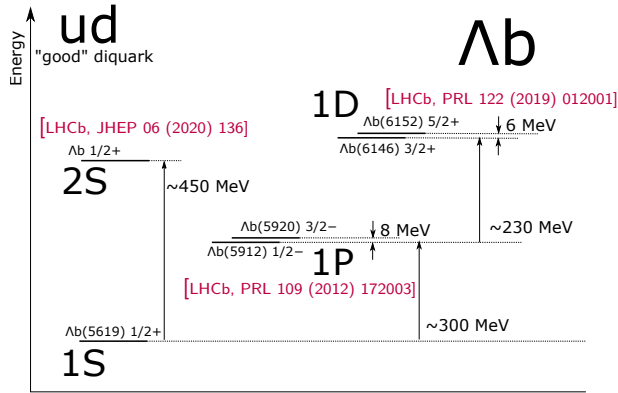
errors: (stat.)(syst.)

# Three-body dynamics in decays of $\Lambda_b^{0**}$

[LHCb, JHEP 06 (2020) 136]

# Excited $\Lambda_b$ resonances

Spectroscopy of the good diquark

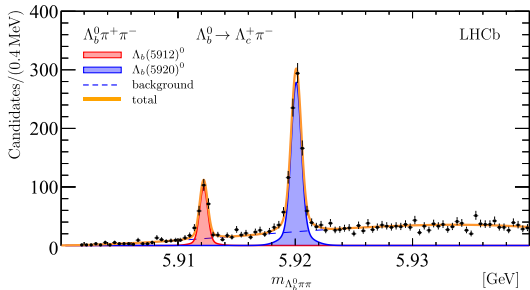


Diquark picture,  $Q(q\bar{q})$  with  $(q\bar{q})$  having  $J^P = 0^+$ , works very well for observed-so-far states.

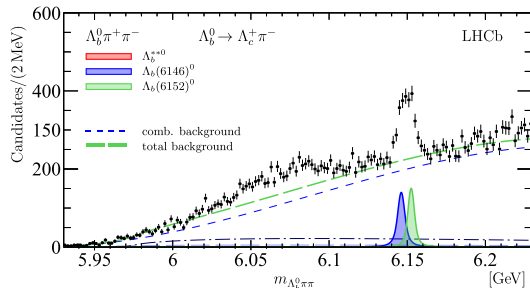
# $\Lambda_b^0\pi^+\pi^-$ spectrum

[LHCb, JHEP 06 (2020) 136]

## Low-mass part of the spectrum



## High-mass part of the spectrum



The broad structure:

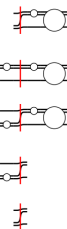
- An elastic resonance in a system  $\Lambda_b^0\pi^+\pi^-$
  - Three coupled quasi-stable channels:  $\Lambda_b^0 f_0$ ,  $\Sigma_b^\pm \pi^\mp$ , and  $\Sigma_b^{*\pm} \pi^\mp$
- ⇒ an excellent opportunity to explore the three-body unitarity

# Three-body unitarity constraint

## Unitarity equation for the reduced amplitude

$$\mathcal{T}(\sigma', s, \sigma) - \mathcal{T}^\dagger(\sigma', s, \sigma) =$$

$$\begin{aligned} & 2i \frac{1}{\lambda_s^{1/2}(\sigma')} \int_{\sigma^-(\sigma', s)}^{\sigma^+(\sigma', s)} d\sigma'_3 t(\sigma'_3) \mathcal{T}(\sigma'_3, s, \sigma) \\ & + \frac{i}{3} \int_4^{(\sqrt{s}-1)^2} \frac{d\sigma''}{2\pi} \mathcal{T}^\dagger(\sigma', s, \sigma'') t(\sigma'') t^\dagger(\sigma'') \rho(\sigma'') \rho_s(\sigma'') \mathcal{T}(\sigma'', s, \sigma) \\ & + 2i \iint_{\phi(\sigma''_2, \sigma''_3, s) > 0} \frac{d\sigma''_2 d\sigma''_3}{2\pi s} \mathcal{T}(\sigma', s, \sigma''_2) t(\sigma''_2) t(\sigma''_3) \mathcal{T}(\sigma''_3, s, \sigma) \\ & + \frac{2i}{3} \frac{1}{\lambda_s^{1/2}(\sigma)} \int_{\sigma^-(\sigma, s)}^{\sigma^+(\sigma, s)} d\sigma_2 \mathcal{T}^\dagger(\sigma, s, \sigma_2) t^\dagger(\sigma_2) \\ & + 6i \frac{2\pi s}{\lambda_s^{1/2}(\sigma') \lambda_s^{1/2}(\sigma)} \theta(\phi(\sigma', \sigma, s)). \end{aligned}$$



Three-main aspects:

- Two-body **rescattering** effects influence of subchannel resonances to each-other lineshape
- Genuine three-to-three dynamics, generated states (**the ladder**)
- Lineshape of the **regular states** decaying to three particles

Related works:

- [Mai et al., EPJA 53 (2017) 9, 177]
- [Jackura et al.(JPAC), EPJC 79 (2019) 1, 56]
- [MM et al.(JPAC), JHEP 08 (2019) 080]

side  
reminder

- A two-body resonance amplitude

$$\hat{\mathcal{R}}(s) = \frac{g^2}{m^2 - s - im\Gamma(s)} = \frac{g^2}{m^2 - s - ig^2\Phi_2(s)/2}$$

$\Phi_2(s)$  is a two-body phase-space

### A resonance in three-body system

#### An approximate-three-body unitarity

$$\hat{\mathcal{R}}(s) = \frac{g^2}{m^2 - s - ig^2/2 \left[ \text{---} \right]}$$

contains effect of the subchannel-resonances interference

#### The quasi-two-body approximation

$$\hat{\mathcal{R}}(s) = \frac{g^2}{m^2 - s - ig^2/2 \left[ \text{---} \right]}$$

naively accounts for the subchannel-resonance decay

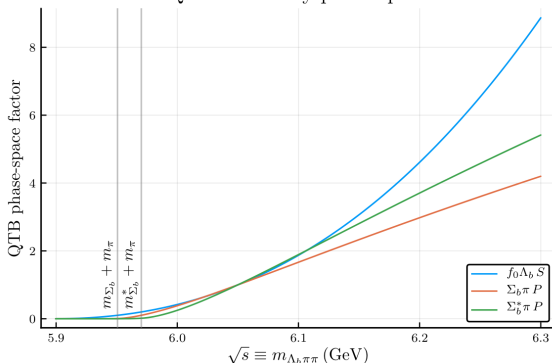
+ dispersion integral to ensure analytic structure (important close to threshold)

# Application to $\Lambda_b^0 \pi^+ \pi^-$ . Self-energy function

$$\rho(s) = \text{diagram} + \text{diagram}$$

$$= \begin{pmatrix} g_{\Lambda_b^0 f_0} \\ g_{\Sigma_b^\pm \pi^\mp} \\ g_{\Sigma_b^{*\pm} \pi^\mp} \end{pmatrix}^\dagger \begin{pmatrix} \Lambda_b^0 f_0 | \Lambda_b^0 f_0 \\ \Sigma_b^\pm \pi^\mp | \Lambda_b^0 f_0 \\ \Sigma_b^{*\pm} \pi^\mp | \Lambda_b^0 f_0 \end{pmatrix} \begin{pmatrix} \Lambda_b^0 f_0 | \Sigma_b^\pm \pi^\mp \\ \Sigma_b^\pm \pi^\mp | \Sigma_b^\pm \pi^\mp \\ \Sigma_b^{*\pm} \pi^\mp | \Sigma_b^\pm \pi^\mp \end{pmatrix} \begin{pmatrix} g_{\Lambda_b^0 f_0} \\ g_{\Sigma_b^\pm \pi^\mp} \\ g_{\Sigma_b^{*\pm} \pi^\mp} \end{pmatrix}$$

Quasi-two-body phase space



$$\sim \sqrt{\text{diagram}} \begin{pmatrix} 1 & z & z_* \\ \cdot & 1+y & x \\ \cdot & \cdot & 1+y_* \end{pmatrix} \sqrt{\text{diagram}}$$

$$\text{with } x(m^2) = -0.014 + 0.004i$$

$$z(m^2) = -0.05 - 0.12i,$$

$$z_*(m^2) = -0.01 - 0.07i,$$

$$y(m^2) = 0.003, \text{ and}$$

$$y_*(m^2) = -0.02$$

$\Rightarrow$  rescattering effects are negligible

# Fit to the data

[LHCb, JHEP 06 (2020) 136]

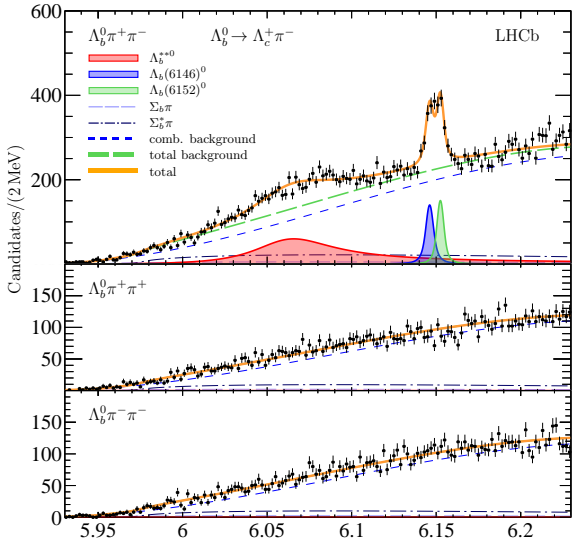
Parameters of the new  $\Lambda_b^0(6072)$ :

$$m = 6072.3 \pm 2.9 \pm 0.6 \pm 0.2 \text{ MeV}$$

$$\Gamma = 72 \pm 11 \pm 2 \text{ MeV}$$

Advance parametrization impacts the width measurement with respect to the naive BW

Framework works  $\Rightarrow$  move to complex examples  $X \rightarrow D\bar{D}\pi(\gamma)$



# Summary

Amplitude analysis is a critical tool for the further progress

Three parts of the three-body problem:

- 3b dynamics – **3b unitarity**
- Angular analysis of the decay – **Dalitz-Plot decomposition**
- Two-body dynamics on the Dalitz – **rescattering** corrections (not covered in this talk)

Wide range of applications of the advanced amplitudes in LHCb. Just two examples:

- Search for CP violation in baryonic decays
- Lineshape analysis for  $\Lambda_b^0$  spectroscopy